Effect of Water Adsorption on Bilayer h-BN: First-Principles Study

G. Paudel, M. Nepal, S. Aryal, A. Devkota and H. K. Neupane

Journal of Nepal Physical Society
Volume 9, Issue 2, December 2023
ISSN: 2392-473X (Print), 2738-9537 (Online)

JNPS, **9** (2): 56-62 (2023)
DOI: https://doi.org/10.3126/jnphyssoc.v9i2.62323

Published by:
Nepal Physical Society
P.O. Box: 2934
Tri-Chandra Campus
Kathmandu, Nepal
Email: nps.editor@gmail.com

JNPS 9 (2): 56-62 (2023)
ISSN: 2392-473X (Print), 2738-9537 (Online)

Research Article *© Nepal Physical Society*
DOI: https://doi.org/10.3126/jnphyssoc.v9i2.62323

Effect of Water Adsorption on Bilayer h-BN: First-Principles Study

G. Paudel[1], M. Nepal[1], S. Aryal[1], A. Devkota[2], and H. K. Neupane[1, *]
[1]Amrit Campus, Tribhuvan University, Kathmandu, Nepal
[2]Central Department of Physics, Tribhuvan University, Kathmandu, Nepal
[*]Corresponding Email: hari.neupane@ac.tu.edu.np

Received: *1st October, 2023;* ***Revised:*** *9th December, 2023;* ***Accepted:*** *24th December, 2023*

ABSTRACT

Recent years have seen a great deal of excitement in the study of the structural, electronic and magnetic behavior of two-dimensional (2D) materials. This has great promise for improved electronics, fascinating quantum technologies, and energy-efficient gadgets. In the current work, we have investigated the structural, electronic, and magnetic properties of bilayer h-BN and water adsorption on pristine h-BN bilayer supercell material using the density functional theory (DFT) method. We have examined the structural properties, and found that they are structurally stable materials. We have examined the band structure and density of states (DoS) calculations of h-BN, and water adsorbed h-BN materials. It is found that water adsorbed on pure h-BN is an n-type Schottky semiconducting material, and pristine h-BN is a broad bandgap p-type Schottky material. P-type insulating material becomes n-type semiconducting material when water molecules are adsorbed. Additionally, after looking the materials' magnetic properties through their DoS and partial density of states (PDoS) analysis. We found that h-BN, and water adsorbed h-BN have non-magnetic properties. Thus, they have been employed extensively in many different industries because of their bandgap energy and non-magnetic in nature.

Keywords: Bandgap, DFT, Fermi-energy, Spin, Symmetry.

1. INTRODUCTION

The two-dimensional (2D) material, hexagonal Boron-Nitride (h-BN) is very similar in structure to graphene. Instead of carbon atoms, it contains Boron (B) and Nitrogen (N) atoms arranged in a hexagonal pattern. This arrangement gives it in-plane trigonal sp^2-bonding, just like graphene. Compared to graphene, h-BN has some distinct advantages. It possesses out-standing mechanical properties and thermal conductivity. Additionally, it is far more stable under high temperatures and harsh chemical conditions. These characteristics make h-BN a superior choice for creating composite materials, especially in hazardous environments [1-3]. Hexagonal-Boron Nitride (h-BN) belongs to a group of III-V compounds. It's essentially a combination of equal amounts of Boron and Nitrogen atoms. Its crystal structure and overall characteristics are quite similar to Carbon. Among III-V semiconductors, h-BN has the wide bandgap, which means, it is a good insulator. It has the ability to be altered through either p-type doping or n-type doping [4-5]. Single-layer hexagonal-Boron Nitride (h-BN) has unique properties due to its structure, including being piezo-electric (it may produce an electric charge under pressure). Remarkably, this feature is absent from the bulk form of hexagonal- Boron Nitride, which consists of stacked layers [6-7]. In h-BN material, there are Boron and Nitrogen atoms arranged in layers with a specific type of bonding network. The bond length between Boron and Nitrogen atoms (B-N) in material is found to be 1.44 Å, which is slightly longer than the bond length between Carbon atoms in graphene (C-C), which is 1.42 Å [8]. There is an existence of weak van der Waals (vdWs) forces between the two layers of hexagonal-Boron Nitride (h-BN) [9-10]. The optical absorption characteristics can indicate the electronic state of the material, which is commonly employed for calculating a semiconductor's bandgap. The available data presents various experiments on h-BN with different structures, revealing a bandgap energy ranging from 3.6 eV to 7.1 eV [11]. Both the direct and indirect characteristics of the bandgap have been included within this range [12]. It possesses a large optical phonon mode, a wide bandgap (4.5 eV in LDA calculations and 6.0 eV in GW calculations), and lacks dangling bonds or electron traps on the surface, classifying it as a wide bandgap insulator [13]. Bulk h-BN has a thermal conductivity that can exceed 400 W/m-k at room temperature. Theoretically, mono-layer 2D h-BN is expected to have a greater thermal conductivity of more than 600 W/m-k [14]. Because of its greater thermal conductivity, the h-BN nanosheets have been utilized as fillers in mineral oil to produce a stable nanofluid for in transformers [15]. The h-BN sheets have a unique property that makes them advantageous for catalytic processes and sensing applications. As a result, they serve as a surface for more effective chemical reactions and can be used to predict certain molecules in their environment. h-BN sheets are useful in a variety of scientific and practical applications because of these characteristics [16-17].

As per our current review of research papers, there is a lack of information regarding the structural, electronic, and magnetic characteristics of pristine bilayer h-BN and water doped on h-BN bilayer supercell structure. Thus, we have used the spin-polarized DFT approach and the Quantum ESPRESSO computational tools to investigate the structural, electronic and magnetic properties of pristine h-BN bilayer supercell structure, and water adsorbed on pristine h-BN bilayer supercell structure.

2. METHODS AND MATERIALS

In the present work, the spin-polarized density functional theory (DFT) under the Quantum ESPRESSO computing tools has been used for the computational of pristine h-BN bilayer supercell and water molecule adsorption on such bilayer supercell structure [18]. To address the exchange-correlation function, we have chosen to use the Predew-Burke-Ernzerhof parameterization (PBE) inside the generalized gradient approximation (GGA) [19]. Ultrasoft pseudopotential (USPP) and plane wave function are utilized in the computations. The interaction between the ion and electron cores is taken into account by USPP [20]. We computed the ideal values for the cutoff kinetic energy (40 Ry) and charge density (400 Ry) in all computations. Systems are permitted to rest after optimization until they attain a total energy convergence threshold of 1.0×10^{-4} Ry and force constant 1.0×10^{-3} Ry/Bohrs. Vanderbilt–Marzari [21] a smearing approach with a degauss value of 0.001 is used for the scf calculations. The band structure calculations are performed using a mesh of (12×12×1), while the density of states (DoS) and partial density of states (PDoS) calculations are performed using a denser mesh of (20×20×1), with 200 k-points used in each calculation. These band structure and DoS calculations are used to predict the electronic properties, DoS and PDoS calculations are used to interpretate the magnetic properties of the materials. XCrySDen and XmGrace software's are used to see the structure visualization and plotting the data for the analysis.

3. RESULTS AND DISCUSSION

In this section, we have interpretated our finding.

3.1. Structural Analysis

First, we built an optimized and relaxed stable unit cell of hexagonal-Boron Nitride (h-BN) structure. We have estimated the distance between the Nitrogen and Boron atoms is 1.45 Ǻ, which is in good agreement with the value that has been reported [22, 23]. The unit cell is extended four times along the x-and y-directions to generate the (4×4) supercell structure of h-BN. There are sixteen Boron and sixteen Nitrogen atoms in one such monolayer of the h-BN supercell structure. The h-BN bilayer is formed by placing the produced monolayer vertically at 3.50 Ǻ. A relaxed calculation is then performed, revealing an interlayer distance of 3.28 Ǻ between these monolayers. The stated values of the other bilayer materials close this value [22, 23]. Figure-1(a) depicts the bilayer h-BN structure, which has 64 atoms total-32 Boron (B) and 32 Nitrogen (N) atoms. Subsequently, we computed the distance between the closest B and N atom, which we discovered to be 1.45 Ǻ, a value that closely matches the published value [22]. The total ground state energy of this system, as assessed by us, is determined to be -852.38 Ry, which is given in Table-3. We deduced from this computation that the h-BN bilayer is a stable structure. According to our estimates, the angle between B-N-B or N-B-N atoms is 119.99^0, the bond length between any two nearest N-N and B-B atoms is 2.38 Ǻ, and the bond length between the nearest B & N atoms is 1.45 Ǻ. These results are shown in Table-1. These approximate values are likewise similar to those of other two-dimensional materials [24-26].

Table 1: Structural properties of pure h-BN

Structural properties of (4×4) pristine h-BN bilayer material	
Bond angle between B-N-B or N-B-N atoms	119.99^0
Bond length between B-N or N-B atoms	1.45 Å
Bond length between N-N or B-B atoms	2.38 Å

The water adsorbed bilayer layer of the h-BN supercell structure has been produced, as the second step. We did relaxed calculations for this by taking a water molecule and placing it at various positions above the top surface of h-BN. Figure-1(b) illustrates the finding that the water molecule is more stable when it is 2.56 Å above the h-BN surface. The total ground state energy of the water adsorbed bilayer h-BN system is also determined by us, and the results is found to be -888.02 Ry. This computation showed that the water-adsorbed hexagonal-Boron Nitride (h-BN) is a stable supercell structure and can be utilized in subsequent operations. Besides these, we have calculated the bond length of it and is found to be 1.45 Å between the nearest B & N atom, the angle of 120.02^0 between the B-N-B or N-B-N atoms, and the bond length of 2.41 Å between any two nearest N-N and B-B atoms. Comparable to previously published results [24-26] are these computed values. The interlayer spacing between h-BN bilayers, which we estimated is 3.29 Å. The value of immaculate h-BN is slightly higher than this. The structural study of the water-adsorbed bilayer of h-BN is supported by estimated parameters, which are shown in Table 2.

Table 2: Structural properties of water adsorbed on bilayer of h-BN

Structural properties of (4×4) water adsorbed h-BN bilayer material	
Bond angle between B-N-B or N-B-N atoms	120.02^0
Bond length between B-N or N-B atoms	1.45 Å
Bond length between N-N or B-B atoms	2.39 Å

Based on the calculations above, we deduced that the pure h-BN bilayer has a slightly more compact structure than the water-adsorbed bilayer h-BN supercell structure. Figure-1(a-b) displays the stable structures of the pure and water adsorbed bilayer h-BN supercell structures respectively.

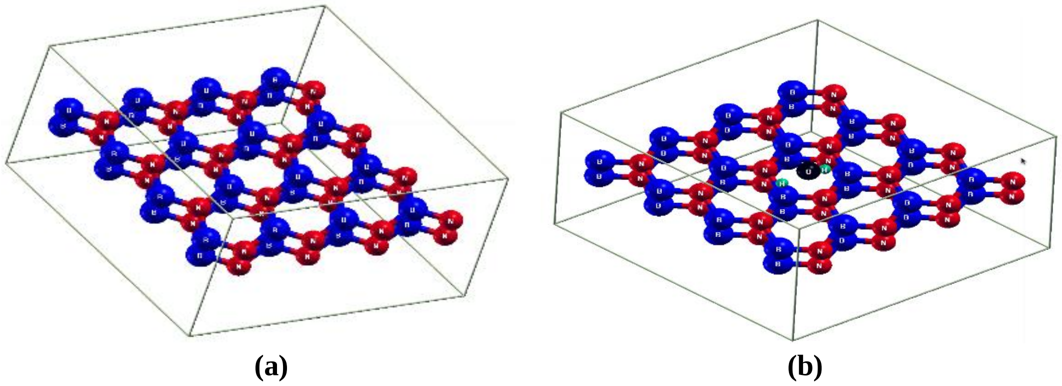

(a) **(b)**

Fig. 1: (Colour online) Optimized and relax structure of pristine and water adsorbed bilayer h-BN materials; (a) h-BN bilayer supercell structure, (b) water adsorbed on h-BN bilayer supercell structure.

3.2. Electronic Properties

The electronic characteristics of the materials under consideration are examined through the examination of their band structures and density of states (DoS) computations. The band structures and DoS of both spin states have been obtained, and they are found to be absolutely symmetrical. Spin-up plots have thus been used by us for additional analysis. Figure 2(a-b) displays the band structure plots of the pristine h-BN bilayer supercell and water adsorbed on pristine h-BN bilayer supercell structures respectively.

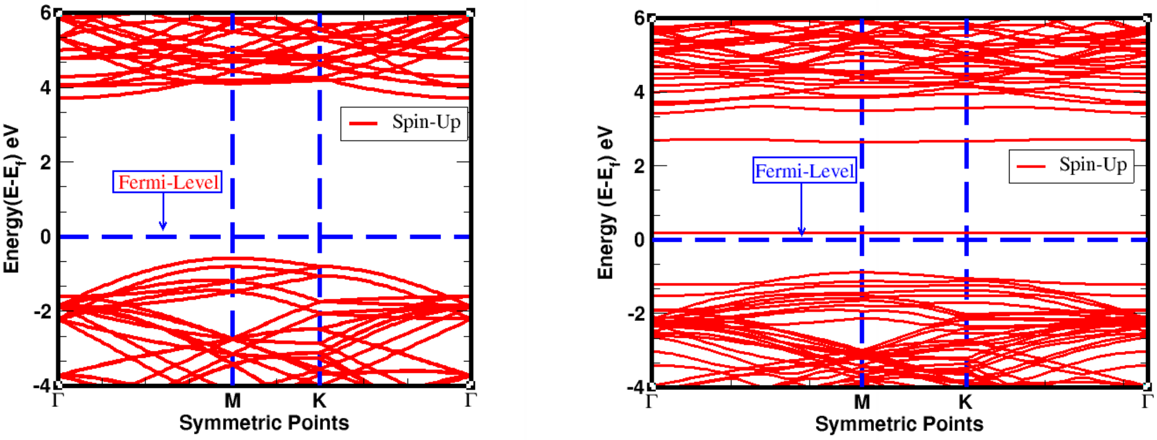

(a) **(b)**

Fig. 2: (Colour online) band structure of; (a) pristine h-BN bilayer supercell structure, and (b) water adsorbed on h-BN bilayer supercell structure.

The x-axis in the above structure signifies the high symmetric points found within the initial Brillouin zone, while the y-axis depicts the associated energy value. The Fermi level serve as a boundary between the valance band and the conduction band, position below the dotted horizontal line is called valance band while the conduction band find above it. The energy difference between these two bands commonly known as bandgap. We have analyzed the band structure of pristine h-BN bilayer supercell structure and found its bandgap energy of value 4.56 eV which is aggregable with the reported value of monolayer h-BN supercell structure [22, 27, 28]. Due to its wide bandgap energy, it is concluded that it is a wide bandgap material. It is seen that band states are appeared more closely in the valence band as compared with that of conduction band. Thus, it has p-type Schottky barrier. Moreover, we have analyzed the band structure plots of water adsorbed h-BN bilayer supercell structure as shown in figure-2(b). It is found that a flat line observed near the fermi level, which is due to the charge transfer, hydrogen bonding, defect and hybridization between water molecule and the h-BN lattice. As a result, its bandgap energy reduced to 1.02 eV. This value is smaller than the bandgap energy value of pristine h-BN bilayer supercell structure. The small bandgap energy value of water adsorbed h-BN bilayer supercell shows that it has semiconducting nature. We have done the self-consistent field (Scf) calculations and found the total energy, Fermi energy, shift of Fermi energy after dopped water molecule, energy of total electrons, Hartree energy, the exchange-correlation, Ewald-energy and the smearing contribution. The computed the value of total ground state energy (E_{tot}) is the sum of energy of total electrons, Hartree energy, the exchange-correlation, Ewald-energy and the smearing contribution. In water adsorbed h-BN bilayer supercell structure, it is observed that Fermi energy level moved towards the valance band by 3.53 eV. This shift shows that there are more holes (electron deficiency) in the valance band. As a result, the Fermi level shift determine the change in the Schottky barrier from being p-type to n-type due to transfer of charge at the interface. Hence, water dopped h-BN bilayer supercell structure has n-type Schottky barrier. We have presented the calculated values of Fermi energy, Fermi energy shift, total energy and bandgap energy of considered material in Table 3.

Furthermore, we have examined the DoS calculations of the materials under consideration and discovered that the bandgap energies of water adsorbed on pure h-BN and pristine h-BN are 1.02 eV and 4.56 eV, respectively. This number further demonstrated that water adsorbed on the pristine bilayer layer of h-BN contains n-type semiconducting material, and that the bilayer layer of h-BN is a large band gap p-type Schottky barrier material. Figure 3(a-b) displays the DoS plots of pristine h-BN bilayer and water adsorbed on pristine h-BN materials respectively.

Table 3: Estimated values of Fermi energy (E_f), Fermi energy shift (E_s), energy of total electrons presented in the structures (e_con), Hartree energy (Har-con), exchange-correlation energy (Xc-con), Ewald energy (Ew-con), total ground state energy (E_t) and total bandgap energy (E_g) of pristine and water adsorbed h-BN bilayer supercell structures.

Considered material/Energy values	h-BN bilayer	Water adsorbed h-BN bilayer
E_f (eV)	-2.27	-1.26
E_s (eV)	-	3.53
e_con (Ry)	-16027.69	-16582.62
Har-con (Ry)	8075.60	8350.55
Xc-con (Ry)	-276.44	386.43
Ew-con (Ry)	7376.14	7630.47
E_t (Ry)	-852.38	-888.02
E_g (eV)	4.56	1.02

3.3. Magnetic Properties

Analysis of the computed density of states (DoS) and partial density of states (PDoS) of the materials under consideration yields predictions about their magnetic characteristics. Figure-4(a-d) displays the DoS and PDoS graphs of the h-BN and water adsorbed on h-BN bilayer supercell structure respectively.

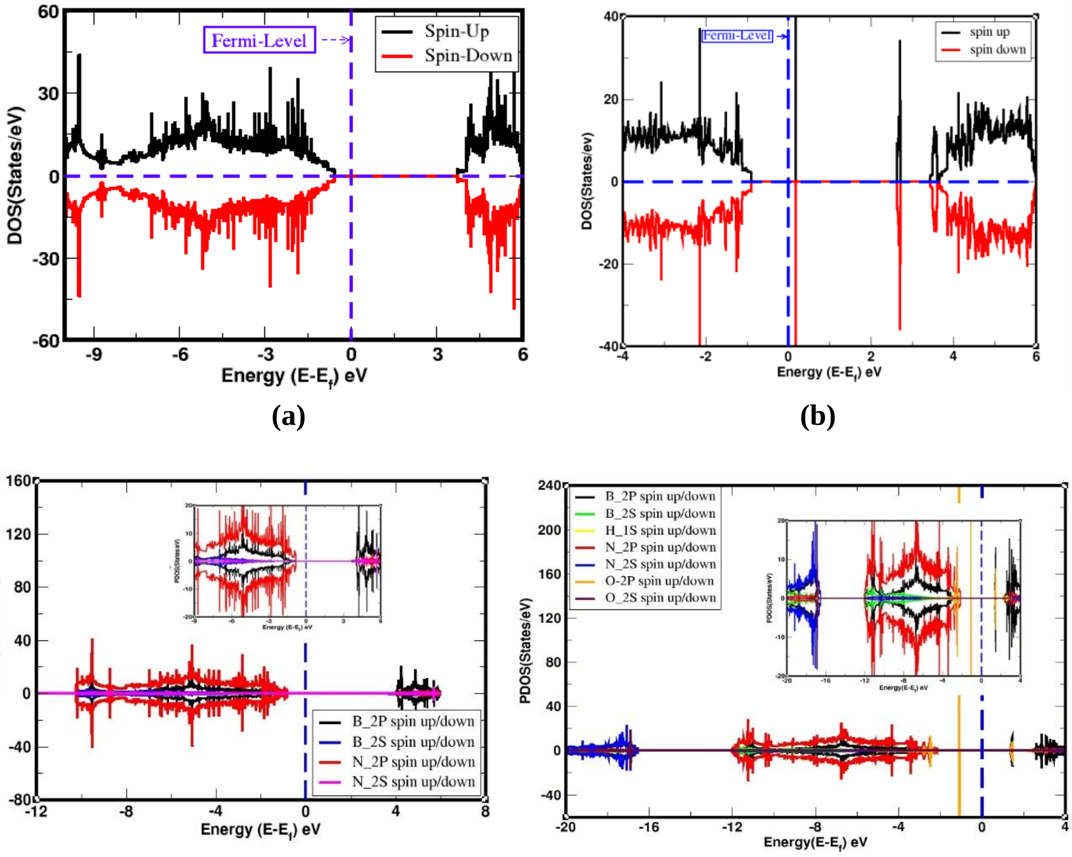

(a) (b)

(c) (d)

Fig. 3: (Colour online) DoS and PDoS plots of: (a) DoS plot of pristine h-BN bilayer supercell structure, (b) DoS plots of water adsorbed on h-BN bilayer supercell structure, (c) PDoS plot of pristine h-BN bilayer supercell structure, (d) PDoS plots of water adsorbed on h-BN bilayer supercell structure. Insets in figure (c-d) represents the zoom scale of PDoS plots].

In figures-3(a-b) represent DoS plots of both spin-up and spin-down of pure and water doped h-BN bilayer supercell structures respectively. Along the y-axis, we display the DoS while corresponding Fermi energy values are presented along the x-axis. The horizontal and vertical dotted lines represent the separation of spin-states, and Fermi energy level respectively. It is found that up-and down-spin states are symmetrically distributed around the Fermi energy level in DoS and PDoS plots. It means, both materials have non-magnetic properties.

According to figure-3(c), Nitrogen's 2p orbitals contribute most to the valence band but very little to the conduction band. Conversely, the valence band is most affected by the 2p orbitals of Boron atoms, which contribute the second most to the conduction band. In the valence band, the Boron 2s orbitals are not very important, but in the conduction band, they are essentially insignificant. The 2p orbitals contribute to the valence band in both Nitrogen and Boron in the energy range of -1 eV to -10 eV. Figure-3(d) illustrates how Oxygen molecules in 2p orbitals produce a sharp vertical line close to the Fermi level, or -1 eV. In the case of Nitrogen, its 2p orbitals have a more substantial impact on the valence band but the least influence on the conduction band. Conversely, Boron's 2p orbitals contribute the second most to the conduction band and the most to the valence band. Boron's 2s orbital plays a minimal role in the valence band and has no contribution to the conduction band. Both Boron and Nitrogen's 2p orbitals contribute within the energy range of -2 eV to -12 eV in the valence band. Despite the differing contributions of orbitals from various atoms, their symmetric structure prevents the development of magnetic properties. Hence both studied materials have non-magnetic properties.

4. CONCLUSIONS

We have investigated the structural, electronic, and magnetic properties of pristine h-BN bilayer supercell structure, and water adsorption on pristine h-BN bilayer supercell structure using spin-polarized density functional theory (DFT) method through Quantum ESPRESSO (QE) computational tools. First, we have studied the structural properties of considered materials by calculating their ground state energies, and found the minimum ground state energies. Hence, they are structurally stable 2D materials. It is also found that pristine form of h-BN bilayer supercell structure is more compact than water adsorption on h-BN bilayer supercell. The materials' electronic properties can be anticipated by examining their band structures and density of states (DoS) plots. The estimated bandgap energy values of water-adsorbed h-BN is 1.02 eV, pristine h-BN is 4.56 eV. They indicate that water adsorbed h-BN is a semiconducting material and pristine h-BN is a wide bandgap material. The p-type wide bandgap material transforms into an n-type semiconducting material upon the adsorption of a water molecule. Furthermore, we have investigated the magnetic properties of pristine and water adsorbed h-BN materials through the analysis of their DoS and PDoS calculations. It is found that up and down spins states are symmetrically distributed around the Fermi energy level which reveals that they have non-magnetic material.

CREDIT AUTHORSHIP CONTRIBUTION STATEMENT

Formal data analysis was used by GP, MN, SA, and AD to generate the data and write the manuscript. The concept was created by HKN, who also oversaw the work, interpreted the data, and evaluated and edited the manuscript.

DECLARATION OF COMPETING INTEREST

The authors hereby certify that they have no known conflicting financial interests or personal connections that could sway the work presented in this publication.

ACKNOWLEDGMENTS

By evaluating the text, the authors would like to thank Prof. NP Adhikari for his outstanding feedback, the Condensed Matter Research Lab, CDP TU, TWAS research grants RG 20-316, and network project NT-14 of ICTP/OE for the computational facilities.

REFERENCES

[1] Neupane, H. K. and Adhikari, N. P. “Tuning structural, electronic, and magnetic properties of C sites vacancy defects in graphene/MoS2 van der Waals heterostructure materials: A first-principles study,” *Adv. Condens. Matter Phys.*, **2020**: 1–11 (2020).

[2] Neupane, H. K. and Adhikari, N. P. “Structural, electronic and magnetic properties of S sites vacancy defects graphene/MoS2 van der Waals

heterostructures: First-principles study," *Int. J. Comput. Mater. Sci. Eng.*, **10** (2): 2150009 (2021).

[3] Golberg, D.; Bando, Y.; Tang, C. C. and Zhi, C. Y. "Boron nitride nanotubes," *Adv. Mater.*, **19** (18): 2413–2432 (2007).

[4] Dahal, R. et al. "Epitaxially grown semiconducting hexagonal boron nitride as a deep ultraviolet photonic material," *Appl. Phys. Lett.*, **98** (21): 2011.

[5] Liu, C. et al. "Single-boron catalysts for nitrogen reduction reaction," *J. Am. Chem. Soc.*, **141** (7): 2884–2888 (2019).

[6] Qi, J.; Qian, X.; Qi, L.; Feng, J.; Shi, D. and Li, J. "Strain-engineering of band gaps in piezoelectric boron nitride nanoribbons," *Nano Lett.*, **12** (3): 1224–1228 (2012).

[7] Duerloo, K. A. N. and Reed, E. J. "Flexural electromechanical coupling: a nanoscale emergent property of boron nitride bilayers," *Nano Lett.*, **13** (4): 1681–1686 (2013).

[8] Lee, K. H. et al. "Large-scale synthesis of high-quality hexagonal boron nitride nanosheets for large-area graphene electronics," *Nano Lett.*, **12** (2): 714–718 (2012).

[9] Jin, C.; Lin, F.; Suenaga, K. and Iijima, S. "Fabrication of a Freestanding Boron Nitride Single Layer and Its Defect Assignments," *Phys. Rev. Lett.*, **102** (19): 195505 (2009).

[10] Nag, A.; Raidongia, K.; Hembram, K. P. S. S.; Datta, R.; Waghmare, U. V. et al. "Graphene Analogues of BN: Novel Synthesis and Properties," *ACS Nano*, **4** (3): 1539–1544 (2010).

[11] Gao, R. et al. "High-yield synthesis of boron nitride nanosheets with strong ultraviolet cathodoluminescence emission," *J. Phys. Chem. C*, **113** (34): 15160–15165 (2009).

[12] Taniguchi, T. and Yamaoka, S. "Spontaneous nucleation of cubic boron nitride single crystal by temperature gradient method under high pressure," *J. Cryst. Growth*, **222** (3): 549–557 (2001).

[13] Wang, J.; Ma, F. and Sun, M. "Graphene, hexagonal boron nitride, and their heterostructures: properties and applications," *RSC Adv.*, **7** (27): 16801–16822 (2017).

[14] Lindsay, L. and Broido, D. A. "Enhanced thermal conductivity and isotope effect in single-layer hexagonal boron nitride," *Phys. Rev. B*, **84** (15): 155421 (2011).

[15] Taha-Tijerina, J. et al. "Electrically insulating thermal nano-oils using 2D fillers," *ACS Nano*, **6** (2): 1214–1220 (2012).

[16] Gao, M.; Lyalin, A. and Taketsugu, T. "Catalytic Activity of Au and Au2 on the h-BN Surface: Adsorption and Activation of O2," *J. Phys. Chem. C*, **116** (16): 9054–9062 (2012).

[17] Lin, Y.; Bunker, C. E.; Fernando, K. S. and Connell, J. W. "Aqueously dispersed silver nanoparticle-decorated boron nitride nanosheets for reusable, thermal oxidation-resistant surface enhanced Raman spectroscopy (SERS) devices," *ACS Appl. Mater. Interfaces*, **4** (2): 1110–1117 (2012).

[18] Giannozzi, P. et al. "QUANTUM ESPRESSO: a modular and open-source software project for quantum simulations of materials," *J. Phys. Condens. Matter*, **21** (39): 395502 (2009).

[19] Perdew, J. P.; Burke, K. and Ernzerhof, M. "Generalized gradient approximation made simple," *Phys. Rev. Lett.*, **77** (18): 3865 (1996).

[20] Troullier, N. and Martins, J. L. "Efficient pseudopotentials for plane-wave calculations. II. Operators for fast iterative diagonalization," *Phys. Rev. B*, **43** (11): 8861 (1991).

[21] Monkhorst, H. J. and Pack, J. D. "Special points for Brillouin-zone integrations," *Phys. Rev. B*, **13** (12): 5188, 1976.

[22] Neupane, H. K. & Adhikari, N. P. "Effect of vacancy defects in 2D vdW graphene/h-BN heterostructure: First-principles study". *AIP Advances*, **11** (8): 2021.

[23] Neupane, H. K. & Adhikari, N. P. "First-Principles Study of Defected Single Layer Hexagonal Boron-Nitride (h-BN)". *Nepal Journal of Science and Technology*, **20** (2): 55-66 (2021).

[24] Lynch, R. W. and Drickamer, H. G. "Effect of high pressure on the lattice parameters of diamond, graphite, and hexagonal boron nitride," *J. Chem. Phys.*, **44** (1): 181–184 (1966).

[25] Sponza, L. et al. "Direct and indirect excitons in boron nitride polymorphs: A story of atomic configuration and electronic correlation," *Phys. Rev. B*, **98** (12): 125206 (2018).

[26] Ooi, N.; Rairkar, A.; Lindsley, L. and Adams, J. B. "Electronic structure and bonding in hexagonal boron nitride," *J. Phys. Condens. Matter*, **18** (1): 97 (2005).

[27] Neupane, H. K. & Adhikari, N. P. "Adsorption of water on C sites vacancy defected graphene/h-BN: First-principles study". *Journal of Molecular Modeling*, **28** (4): 107 (2022).

[28] Neupane, H. K.; Bhattarai, B. & Adhikari, N. P. "Transport properties of B and N sites vacancy defects graphene/h-BN heterostructures: First-principles study". *Physica B: Condensed Matter*, 415077, 2023.